ELECTRON HEAT CONDUCTIVITY AND THE WIEDEMANN-FRANZ LAW FOR Bi

I. Ya. KORENBLIT, M. E. KUZNETSOV, V. M. MUZHDABA, and S. S. SHALYT

Institute of Semiconductors, USSR Academy of Sciences; A. F. Ioffe Physico-technical Institute, USSR Academy of Sciences; Leningrad Pedagogical Institute

Submitted January 31, 1969

Zh. Eksp. Teor. Fiz. 57, 1867–1876 (December, 1969)

The heat conductivity of the current carriers in Bi has been determined by a study of the effect of a strong classical magnetic field on the total thermal conductivity of the crystal. In this way the Lorentz number and the Wiedemann-Franz law could be determined. At T = 80–100°K, the Lorentz number corresponds to elastic scattering. The value of the Lorentz number at T < 30°K indicates the inelastic character of the scattering of the carriers. An analysis showed that the inelasticity due to intravalley scattering by acoustic phonons is small and cannot explain the experimental results. The observed inelasticity may be due to intervalley scattering by the current carriers or to their mutual scattering.

INTRODUCTION

THE parallel measurement of the electrical conductivity (σ) and the electron heat conductivity (κ_0) of a conductor allows us to determine the Lorentz number L in the Wiedemann-Franz law: $\kappa_0/\sigma T = L$. Subsequent comparison of the experimental value of the Lorentz number with its theoretical value for different electron models of a conductor can serve as a source of information on the spectrum of the carriers and on the mechanism of their scattering in a crystal. Information on the second problem is especially important, since other known experimental approaches to its solution frequently lead to ambiguous conclusions. Analysis of the Wiedemann-Franz law at least allows us to carry out a review of the possible scattering mechanisms in the conductor under study. If we are dealing with semiconductors and semimetals, for which phonons make a contribution to the thermal conductivity along with electrons, then the question arises as to the method of separate determination of the electron and phonon components of the heat conductivity of such a conductor. The effect demonstrated by a strong transverse magnetic field on the total heat conductivity K_0 can be used as such a method.

We have in mind the classical case of a strong field $uH/c \gg 1$ (u is the mobility), which, because of the rather high temperature T of the experiment ($k_0T \gg \hbar eH/m^*c$), does not produce any characteristic quantum effects.

In the analysis of the heat conductivity of Bi, it is necessary to remember that electrons and holes enter into the composition of its carriers in equal concentrations, and therefore, even in a limitingly strong magnetic field, the electron component of its heat conductivity is not completely suppressed. The remaining part of this heat conductivity (as $H \to \infty$) can be determined from theoretical formulas, which contain components of galvanomagnetic (ρ_{ij}) and thermomagnetic (α_{ij}) tensors of Bi, which can be suitably determined experimentally.

If the coordinate axes 3 and 1 are directed along the trigonal and binary axes of the crystal, while the axis 2 is perpendicular to 3 and 1 and is directed along the bissectrix direction, then the formulas for the remaining electron heat conductivity along the two fundamental directions of the Bi crystal have the form (see the Appendix):

$$\varkappa_{33}(H \to \infty) = \delta\varkappa_{33} = T\frac{\alpha_{23}^2\rho_{33} + \alpha_{33}^2\rho_{22} - 2\alpha_{33}\alpha_{23}\rho_{23}}{\rho_{22}\rho_{33} - \rho_{23}\rho_{32}}, \quad (1)$$

$$\varkappa_{11}(H \to \infty) = \delta\varkappa_{11} = T\frac{\alpha_{12}^2}{\rho_{11}}. \quad (2)$$

Still another circumstance is associated with the bipolar nature of the current carriers in Bi; this must be kept in mind in the analysis of its heat conductivity.[1] In contrast with the electric conductivity ($\sigma = \sigma_e + \sigma_h$), the total heat conductivity of the electrons and holes is not an additive quantity, and contains a component which is determined by bipolar thermal diffusion:

$$\varkappa_0 = \varkappa_e + \varkappa_h + T\frac{\sigma_e\sigma_h}{\sigma_e + \sigma_h}(\alpha_h - \alpha_e)^2. \quad (3)$$

During the past forty years, a number of researches have been published in which the analysis of the heat conductivity of Bi at low temperatures has been carried out by the method of a strong magnetic field,[2] but none of them took into account, whether wholly or in part, those special features of this method which were discussed in connection with Eqs. (1), (2), and (3).

In[3], the total electron heat conductivity and its components, which appear in Eq. (3) (for the interval T = 80–300°K), were calculated on the basis of known data on the partial values of the concentration, mobility and chemical potential of electrons and holes, which were obtained by analysis of a large amount of experimental results. The lattice component of the heat conductivity was calculated here as the difference between the experimentally measured value of the total heat conductivity K_0 and the computed value κ_0. In the present work, the values of the total heat conductivity of the crystal K_0 and its lattice component K were measured experimentally, while the value of the electron component was computed from the difference of the experimental heat conductivities $\kappa_0 = K_0 - K_l$. After giving the experimental results, we shall make a comparison of the results of the determination of κ_0 here for two different approaches to the analysis of the heat conductivity of Bi.

EXPERIMENTAL RESULTS AND THEIR DISCUSSION

The value of the heat conductivity was determined by the method of stationary heat flow between the sample, soldered to the end of a vacuum chamber and placed in a liquid thermostat (nitrogen, oxygen, helium). Carbon resistors served as thermometers for the range 2°–40°K and copper-constantan thermocouples for the range T > 40°K. The thermal emf of the studied samples was measured in relation to copper. The length of the single crystals exceeded 50 mm, the transverse dimensions amounted to 1.5–4 mm.

Figure 1 shows some typical curves for the dependence of the change in the total heat conductivity of the crystal ΔK_0 on the magnetic field intensity H. In single crystals of pure Bi, because of the high mobility of the current carriers, complete saturation was achieved in all cases.

Figure 2 shows the principal results of the investigation of the heat conductivity of pure Bi. Two of the studied single crystals of longitudinal ($\nabla T \parallel C_3$) and transverse ($\nabla T \perp C_3$) orientation had resistance ratios $\rho_{300°K}/\rho_{4.2°K}$ of 230 and 390, respectively and diameters of 2.56 and 2.65 mm, respectively. The electron heat conductivity was determined as a sum: $\kappa_0 = K_0(H \to \infty) + \delta\kappa$. The first component gave curves of the type shown in Fig. 1, and the second was determined from Eqs. (1) and (2). The upper two curves (7 and 8) characterize the anisotropy of the total and the lattice heat conductivities of the crystal. Curves 3 and 4 show how the total electron heat conductivity of Bi(κ_0) changes with temperature along the two principal directions of the crystal. Curves 5 and 6 show how the relative fraction of these two components of the electron heat conductivity changes with temperature.

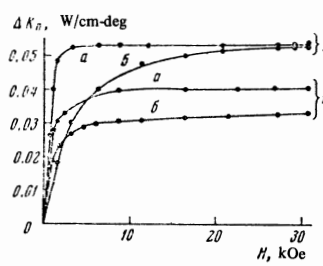

FIG. 1

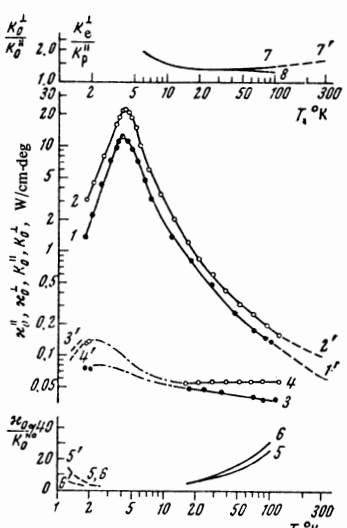

FIG. 2.

FIG. 1. Typical curves for the dependence of the change of the total heat conductivity on the magnetic field intensity for different temperatures in single crystals of pure Bi of two orientations: 1 – $\nabla T \parallel C_3$, 2 – $\nabla T \perp C_3$; a – T = 27°K, b – T = 95°K

FIG. 2. Temperature dependence of the total $K_0^{\parallel,\perp}$ (1,2) and electron $\kappa_0^{\parallel,\perp}$ (3,4) heat conductivities of pure Bi single crystals: 1 and 1′ for $\nabla T \parallel C_3$, 2 and 2′ for $\nabla T \perp C_3$; dashed parts 1′, 2′, 7′ are taken from [7]; 3 and 3′ for $\nabla T \parallel C_3$; 4 and 4′ for $\nabla T \perp C_3$; dashed parts of 3′, 4′, 5′, 6′ are computed by us from the data of [8]; 5 and 6 – relative values of κ_0/K_0 for $\nabla T \parallel C_3$ and $\nabla T \perp C_3$; 7 and 8 – anisotropies of the total and lattice heat conductivities.

Our experimental data were obtained in the temperature range 2–100°K. The dashed curves 3′, 4′, 5′, 6′ for the range 1.8–1.3°K were computed by us from the experimental data of [4]. A certain lack of agreement of curve 3′ and 4′ with our curves 3 and 4 can be attributed to the difference in the purities of the crystals, which has a strong effect on the heat conductivity of Bi in this range of temperatures (below 3°K). It is essential that curves 3′ and 4′ have the form expected for the region of very low temperatures, when the heat conductivity of the electrons is fundamentally determined by a heat capacity that decreases with temperature. In the range of temperatures 10–100°K, the increase in the heat capacity of the electrons with temperature is almost neutralized by the decrease occurring in the length of the free path. Curves 5 and 6 of the lower part of Fig. 2 show that the relative part of the electron heat conductivity of Bi, which becomes a difficult quantity to measure for T < 20°K, increases up to entirely measurable values for T < 3°K and increases rapidly with further decrease in the temperature.

1. HIGH TEMPERATURES: 80–100°K

After finding the electron heat conductivity of the conductor, one must analyze the Wiedemann-Franz law $\kappa_0/\sigma T = L$. As was pointed out above, a comparison of the experimental value of the Lorentz number with the theoretical value can be the source of important information on the current carriers and heat carriers in the crystal. The data on the electric conductivity σ of the single crystals studied, which are needed for this analysis, are shown in Fig. 3. The experimental data for the Lorentz number for T > 2°K along the two principal directions of the bismuth crystal, $L_\perp$ and $L_\parallel$ are shown in Fig. 4. It was shown above that in [4] there are all the necessary experimental data for the calculation of κ_0 below 2°K, and consequently, all that is needed for the calculation of L. For the single crystals of Bi, No. 7 and No. 4, studied in [4] for the temperature range 1.3–1.8°K, the values obtained for $L_\perp$ and $L_\parallel$ were close to 2×10^{-8} V^2-deg^{-2}.

It is seen from Figs. 2, 3, and 4 that for T = 80°K, the anisotropy of σ does not amount to 10%, while the anisotropy for κ_0 and L exceed 40 and 30%, respectively.

From Eq. (3), one can obtain an expression for the total Lorentz number

$$\frac{\varkappa_0}{\sigma T} = L = \frac{L_e}{1+\sigma_h/\sigma_e} + \frac{L_h}{1+\sigma_e/\sigma_h} + \frac{\sigma_e\sigma_h(\alpha_h-\alpha_e)^2}{(\sigma_e+\sigma_h)^2}, \quad (4)$$

where $L_{e,h} = \kappa_{e,h}/\sigma_{e,h}T$ are the partial Lorentz numbers for electrons and holes, which depend on the reduced chemical potential $\mu^* = \mu/k_0T$, the scattering mechanism and the dispersion law. If the dependence of the relaxation time on the energy is the same for all directions of the crystal, then L_e and L_h are isotropic quantities. The numerical values of σ_e, σ_h, α_e, α_h, μ_e, and μ_h are given in [3]. The partial thermal emfs α_e and α_h are isotropic and the factors $\sigma_h\sigma_e$ in the third component of Eqs. (3) and (4) differ by a factor of three for the two principal directions of the bismuth crystal ($\perp$ and $\parallel C_3$). The anisotropies of κ_0 and L are

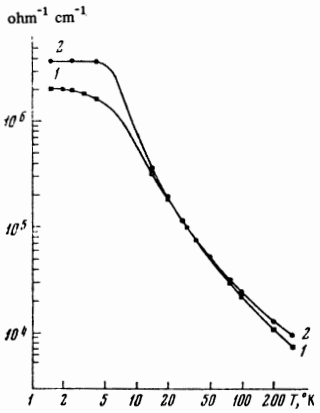

FIG. 3

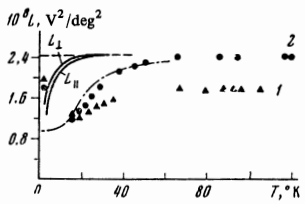

FIG. 4

FIG. 3. Temperature dependence of the specific electrical conductivity for the two principal directions of the Bi crystal: 1 – j ∥ C_3, 2 – j ⊥ C_3.

FIG. 4. Experimental results of the determination of the Lorentz number for 1 – ∇T ∥ C_3; 2 – ∇T ⊥ C_3. The solid lines represent the results of calculation. The dashed line is the Sommerfled value. The dot-dash line represents the result of calculation from the formula (11).

connected with these very components, which determine the contribution of thermal diffusion in (3) and (4).

The difference $L_\perp - L_\parallel = 0.53 \times 10^{-8}$ V²-deg⁻², computed with the help of data on the partial values of σ, α, and μ, given in[3], is in excellent agreement with the experimental value of this difference, which is shown in Fig. 4 (0.55×10^{-8} V²-deg⁻²).

By solving two equations of type (4) for $L_\perp$ and $L_\parallel$ at the values of the total Lorentz number $L_\perp$ and $L_\parallel$ known from experiment, we obtain: $L_e = 1.5 \times 10^{-8}$ V²-deg⁻², $L_h = 1.45 \times 10^{-8}$ V²-deg⁻². In[3], the partial values L_e and L_h were computed from the given values of the chemical potential under the assumption of a quadratic dispersion law and scattering of the current carriers by acoustical phonons. The values of $\kappa_0^\perp$ and $\kappa_0^\parallel$ computed in this way were higher by 30% than our experimental values. It is of interest to determine the reason for such a divergence in this region of temperatures, which are comparatively high for Bi, where the scattering is thermal and where the individual properties of the samples, determined by the amount of impurities and defects, do not come into play. Analysis has shown that if, following the method of[3], we compute L_e and L_h with account of the nonparabolic character of the bismuth spectrum, under the assumption of elastic scattering, we obtain the values $L_e \approx L_h \approx 1.5 \times 10^{-8}$ V²-deg⁻², which agrees with the values obtained from our experimental data. The nonparabolic character of the spectrum has practically no effect on the difference $\alpha_e - \alpha_h$ which enters in (4).

2. LOW TEMPERATURES: T < 30°K

We now consider the region of temperatures in which the electrons and holes in bismuth are strongly degenerate. As is known ([5], p. 346; [6]), for degenerate carriers, the Lorentz number takes on the Sommerfeld value $L_0 = \pi^2 k_0^2/3e^2 = 2.44 \times 10^{-8}$ V²-deg⁻², if the scattering is elastic (independent of the structure of the spectrum), and deviates from the Sommerfeld value of inelastic scattering. It is seen from Fig. 4 that the experimental value of the Lorentz number for T ≲ 30°K differs appreciably from the Sommerfeld value; consequently, in this range of temperatures in bismuth, the inelastic scattering of the current carriers plays a significant role.

In principle, the following inelastic mechanisms of scattering are possible: 1) intravalley scattering by phonons; 2) intervalley scattering by phonons; 3) inelastic scattering by impurities; 4) mutual scattering of current carriers. We now proceed to the analysis of each of these mechanisms. For this, we shall take into account not only our data, but also the experimental data on the temperature dependence of the electrical resistivity of pure bismuth, obtained by other authors.

1. We first consider the scattering by acoustical phonons. In the case considered by us of strongly degenerate carriers with ellipsoidal nonparabolic dispersion law

$$\gamma(\varepsilon) = \sum_l \frac{p_l^2}{2m_l} \tag{5}$$

it is not difficult, in the usual fashion[5], to obtain the following expressions for the diagonal components (in the axes of the mass ellipsoid) of the tensors of electrical resistivity ρ_{ll} and thermal resistivity λ_{ll}:

$$\rho_{ll} = \frac{9m_l}{32\pi e^2 \gamma_F} \sum_{\mu=1}^{3} \int W_f^{(\mu)} \xi_\mu(f) F(\xi_\mu) f_l^2 \frac{d^3 f}{f}, \tag{6}$$

$$\lambda_{ll} = \frac{27 m_l}{32\pi^3 \hbar^2 T \gamma_F} \sum_{\mu=1}^{3} \int W_f^{(\mu)} F(\xi_\mu) \xi_\mu(f) \left[\left(1 - \frac{f^2}{4} - \frac{f_l^2}{f^2} + \frac{5}{12} f_l^2 \right) \frac{3\xi_\mu^2}{2\pi^2} + f_l^2 \right] \frac{d^3 f}{f}, \tag{7}$$

with f ≤ 2. Here $\gamma_F = \gamma(\epsilon_F)$, $f_l = q_l/\sqrt{2m_l \gamma_F}$, q is the momentum of the phonon, $\xi_\mu(f) = \hbar \omega_q^{(\mu)}/k_0 T$, $\omega_q^{(\mu)}$ is the frequency of the phonon of polarization μ, $W_f^{(\mu)} = (2\pi/\hbar)$ multiplied by the square of the modulus of the matrix element of the transition,

$$F(\xi_\mu) = (e^{\xi_\mu} - 1)^{-1} (1 - e^{-\xi_\mu})^{-1}. \tag{8}$$

In order to proceed further, it is necessary for us to know the spectrum of phonons interacting with the electrons, and the magnitude of this interaction. The maximum Fermi momentum of the electrons in bismuth is $P_{max} = (7.6 \pm 0.3) \times 10^{-21}$ g-cm/sec².[7] Consequently, acoustical phonons with wave vectors less than $q_{max} = 2P_{max}/\hbar = 1.5 \times 10^7$ cm⁻¹ interact with the electrons. This value is four or five times smaller than the limiting wave vector. From neutron diffraction studies of the phonon spectrum of bismuth,[8] it follows that for such small wave vectors, the acoustical branch of the spectrum does not possess dispersion. The maximum Fermi momentum of the holes is less than that of the electron, and correspondingly less is the wave vector of the phonons interacting with them.

It is still necessary to consider the following. The total resistance of the bismuth is obtained by summation of the partial resistances pertaining to the separate ellipsoids. Since the components of the partial resistance along the minor axes of the ellipsoid is less than along the major axis, then these give the principal con-

tribution to the total resistance. But the phonons with q_{max} do not participate in the components of the resistance along the smaller axes, so that actually we are dealing with phonons whose wave vectors are still less than q_{max}.

Consequently, it is possible to use the spectrum of acoustical phonons in bismuth, which is established approximately in[9] from experimental elastic constants, and the interaction of the carriers with the phonons is computed within the framework of the model of the deformation potential. In the calculation of the electrical resistivity ρ and the Lorentz number L for electrons, the following simplifications were also made: the real phonon spectrum is approximated by an isotropic one, and the spectrum of electrons by a system of three ellipsoids of rotation, the axes of which coincide with the crystallographic axes; the axis of rotation (the major axis) is parallel to the twofold axis. One can show that errors brought about by the given approximation of phonon and electron spectra compensate one another to a considerable degree. As we shall see below, these simplifications are admissible for the given problem.

Numerical calculations were carried out on the BESM-3 high-speed computer. We used the following parameters: masses of holes and electrons in units of the mass of the free electron[10] $m_1^h = m_2^h = 0.0677$, $m_3^h = 0.758$, $m_1^e = 0.00709$, $m_2^e = 1.71$, $m_3^e = 0.0115$. The Fermi energies[11]: $\epsilon_F^e = 26$ MeV, $\epsilon_F^h = 11$ MeV. The constants of the deformation potential[12]: $D_{33}^h/D_{22}^h = -1.03$; $D_{33}^h = \pm 1.2$ eV; $D_{11}^e/D_{22}^e = -0.37$; $D_{33}^e/D_{22}^e = -0.29$; $D_{22}^e = \pm 5.9$ eV. The elastic constants were taken from[13].

Figure 4 shows the theoretical dependence of the Lorentz number on the temperature, due to the inelasticity of the phonon scattering. It is seen that in the range 10–30°K L_{th} is much greater than the experimental L and consequently the considered mechanism is not the basic mechanism of scattering in bismuth at low temperatures T. Analysis of the electrical resistivity supports this conclusion.

In superpure samples for $T < 30°K$, $\rho \sim T^2$ [4,14-17] but the resistivity computed by us should have such a curve only for $T < 5°K$; the transition from the quadratic dependence of $\rho(T)$ to the linear takes place in the range 5–20°K. The theoretical value of ρ was shown to be significantly less than the experimental: for $T = 10°K$, $\rho_{\parallel}^{theor} = 2.4 \times 10^{-7}$ ohm-cm while $\rho_{\parallel}^{exp} = 1.2 \times 10^{-6}$ ohm-cm.[14] The divergence of the theoretical and experimental results is so significant that it is not possible to explain them by simplifications made in the calculation of the electrical and thermal resistivities.

The role of optical phonons in the intravalley scattering is more difficult to set forth, since the energy of coupling of the phonons with the carriers is unknown to us. The minimum energy of the optical phonons is 100°K according to[8]. One can therefore expect that their contribution is unimportant for $T \lesssim 20°K$.

2. Intervalley scattering in bismuth can take place from phonons with limiting wave vectors. According to[8,16], the energy of such phonons in the direction ΓX (Γ is the center of the Brillouin zone, Z the center of the rectangle bounding the zone[7]) amounts at most to $\hbar\omega_0 \approx 40°K$. It was shown in[16] that the phonons of ΓX can cause the transition of electrons between the electron and hole ellipsoids, while the symmetry allows the participation of such a phonon in this process. It is not difficult to see that transitions between electron ellipsoids can also exist for the phonons of ΓX.[1)] Thus, the intervalley scattering can be important at the temperatures $T < 30°K$ of interest to us; therefore, it is necessary to consider this mechanism in detail.

Since phonons with momenta much greater than the intravalley momenta of the carriers take part in the intervalley scattering, the scattering probability does not depend on the initial and final states of the carriers. This circumstance allows us to describe such processes with the help of the relaxation time.[18] A simple generalization of the Herring theory to the case of degenerate statistics of carriers with Fermi energies $\epsilon_F \gg \hbar\omega_0$ gives the relation

$$\frac{1}{\tau(\varepsilon_1)} = W g_2(\varepsilon_1) \operatorname{cth} \frac{\hbar\omega_0}{2k_0T} \frac{n(\varepsilon_1 + \hbar\omega_0) n(\varepsilon_1 - \hbar\omega_0)}{n^2(\varepsilon_1)}, \qquad (9)$$

for the relaxation time of the carriers of ellipsoid 1 scattered into ellipsoid 2. Here $W = 2\pi\hbar^{-1} \times$ the square of the modulus of the transition matrix element, $g_2(\epsilon)$ is the density of states of the ellipsoid 2, and $n(\epsilon)$ is the Fermi distribution function.

For the i-th component (in terms of the axes of the ellipsoid 1) of the electrical conductivity $\sigma_{ii}(1 \rightharpoonup 2)$ and the Lorentz number L, we have

$$\sigma_{ii}(1 \rightharpoonup 2) = \frac{2n^{(1)}e^2}{3m_i} \frac{1}{W g_2(\varepsilon_F)} \operatorname{th} \frac{\hbar\omega_0}{2k_0T} \left(1 + \frac{1}{2} \operatorname{ch} \frac{\hbar\omega_0}{k_0T}\right), \qquad (10)$$

$$L = L_0 \left(1 - \frac{6}{\pi^2} \frac{\operatorname{ch}(\hbar\omega_0/k_0T) - 1}{\operatorname{ch}(\hbar\omega_0/k_0T) + 2}\right), \qquad (11)$$

where $n^{(1)}$ is the carrier concentration in ellipsoid 1, and m_i is the mass of the carriers in the direction i.

The deviation of the Lorentz number from the Sommerfeld value in inelastic scattering is connected with the fact that the relaxation time (5) changes rapidly with ϵ in the region $\epsilon - \epsilon_F \approx k_0T$, so that it is not possible to replace $\tau(\epsilon_F)$ for $\tau(\epsilon)$ in the calculation of the electrical conductivity and heat conductivity.

For $\hbar\omega_0/k_0T \gg 1$ we have $L/L_0 = 1 - 6/\pi^2$; with increase in temperature, L slowly approaches L_0. If we take $\hbar\omega_0 = 43°K$,[16] then the (isotropic) values of L computed from (11) will be sufficiently close to the values observed by us experimentally (Fig. 4). Thus our experimental results can be explained by intervalley scattering. In order to explain whether this scattering mechanism is actually decisive, it is necessary to establish what its contribution is to the electrical resistivity (heat resistivity). If we calculate $\sigma_{ii}(1 \rightharpoonup 2)$ from (10), using the constant W from[16] for transitions from the electron to the hole ellipsoid, then it is shown that the total resistivity (summed over all ellipsoids) determined by this mechanism is much less than the experimental one. Thus the computed resistivity along the trigonal axis is equal to 7×10^{-8} ohm-cm for $T = 10°K$ and 10^{-6} ohm-cm for $T = 30°$, while experiment[14] gives 1.2×10^{-6} and 10^{-5} ohm-cm, respectively.

[1)] We have not made clear what hindrances the symmetry conditions impose on this process.

In the same way, using the corresponding constant from[16], we can establish the fact that the intervalley scattering with participation of optical phonons also gives a small contribution to the resistivity for $T < 30°K$. However, it is not possible to consider the value of the constants from[16], used by us, as solidly established. Moreover, the contribution to the resistivity of the transitions between the electron ellipsoids is not known. Therefore, it is not excluded that the intervalley scattering in Bi is important in the temperature region considered.

3. So far as we know, there are no data at the present time on impurity levels in bismuth which can cause inelastic scattering; therefore, a detailed analysis of the third of the mechanisms indicated above is impossible. We note only that the departure from the Sommerfeld value is observed at temperatures at which the impurity scattering does not play any significant role (if we evaluate it from the temperature dependence of $\rho(T)$). Therefore, this mechanism can scarcely be the reason for inelastic scattering of the carriers.

4. Finally, we consider the scattering of the carriers by carriers, which, as is known, give the experimentally observed quadratic dependence of ρ on T.

In bismuth, the electron-electron scattering cannot give a contribution to the electrical resistivity since there is no transport process. The source of electrical resistance can be electron-electron scattering, since the electrons and holes move in opposite directions in the electric field. We initially estimate the value of this resistance by using the formula for resistance in the scattering of s-electrons by the heavy d-electrons in the transition metals ([5], p. 373):

$$\rho \approx \frac{e^2 (m_h^*)^2}{\chi_0 n \hbar^3} \frac{p_F r_0}{\hbar} \left(\frac{T}{\varepsilon_F^e} \right)^2. \qquad (12)$$

Here χ_0 is the dielectric constant, n the concentration of electrons, $r_0 = \sqrt{\epsilon_F \chi_0 / 6\pi e^2 n}$ the screening radius, and m_h^* the mass of the density of states of the holes. For bismuth, $\chi_0 = 100$[7], $r_0^{-1} \approx 5 \times 10^5$ cm^{-1}, $p_F/\hbar = (3\pi^2 n)^{1/3} \approx 2 \times 10^6$ cm^{-1}, so that for $T = 10°K$, we have $\rho \approx 10^{-5}$ ohm-cm, which is almost an order of magnitude greater than the experimental value of ρ.

In order to verify whether there is significant error in the application to bismuth of the formula obtained for the isotropic spectrum of the carriers, we studied the anisotropy of the spectrum of holes and electrons, where we used the previously described simplified spectrum for electrons. For simplicity, it was assumed that the holes were in equilibrium and made no appreciable contribution to the current. This is valid for the resistance in the direction of the trigonal axis, since $m_3^h \gg m_3^e$. Here we obtained

$$\rho_{\perp} \approx \frac{e^2 (m_h^*)^2}{n \chi_0^2 \hbar^3} \left(\frac{m_1^e}{m_3^e} \right)^{1/4} \frac{r_0}{\hbar} \sqrt{2 m_1^e \varepsilon_F^e} \left(\frac{T}{\varepsilon_F^e} \right)^2 \approx \qquad (13)$$

$$\approx 2 \cdot 10^{-6} \text{ ohm-cm for } T = 10°K$$

which is in satisfactory agreement with the experimental value.[14]

In addition to electron-hole scattering, the scattering of electrons by electrons and holes by holes also make contributions to the heat resistance. For this reason, the Lorentz number can be less than the Sommerfeld value. However, the complicated character of the spectrum makes any reliable estimate of the Lorentz number difficult in this case.

Thus a comparison of the experimental data with the theory allows us to conclude that the scattering of the current carriers in pure Bi at low temperatures ($T < 30°K$) has an inelastic character. It seems that the reason for this inelasticity can be either intervalley scattering of carriers by phonons, or the scattering of carriers by carriers, or by the simultaneous action of both mechanisms.

In conclusion, the authors express their gratitude to A. S. Skal for help in the computer calculations, to V. I. Pol'shin for help in the measurements, to Yu. M. Kagan for a number of valuable critical remarks, L. L. Kornblit, and Yu. I. Tavich for the discussion of certain theoretical questions, and to I. E. Galkina and L. B. Bezymenskii for preparation of the single crystals of bismuth.

APPENDIX

From the phenomenological expressions for the electric field and heat flow

$$j_i = \sigma_{ik}(H) E_k + d_{ik}(H) \frac{\partial T}{\partial x_k}, \quad q_i = c_{ik}(H) E_k - \gamma_{ik}(H) \frac{\partial T}{\partial x_k} \qquad (A.1)$$

and the Onsager relations, it follows that the heat conductivity, which is determined by the relation $q_i = -\kappa_{ik}(H) \partial T / \partial x_k$, at $j = 0$ is expressed by the kinetic coefficients entering into (A.1) in the following way:

$$\varkappa_{kn}(H) = \gamma_{kn}(H) - T \alpha_{ik}(-H) \sigma_{lm}(H) \alpha_{mn}(H), \qquad (A.2)$$

where the thermal emf $\alpha_{lk}(H) = -\rho_{li}(H) d_{ik}(H)$, $\rho_{li}(H)$ is the electrical resistivity tensor, $\gamma_{kn}(H)$ an additive quantity. As $H \to \infty$, the electron and hole contributions to γ_{kn} vanish and the second component in (A.2) generally does not approach zero. If $H \parallel C_3$, then

$$\alpha_{21}(-H) = \alpha_{12}(H), \quad \alpha_{23}(H) = \alpha_{13}(H) = 0$$

and as $H \to \infty$, $\alpha_{11} = \text{const}$, $\alpha_{12} H \propto H$, $\sigma_{11} \propto H^{-2}$, $\sigma_{12} \propto H^{-3}$, so that the formula (2) reduced to basic form, follows from (A.2). For $H \parallel C_2(Ox)$, as a consequence of rotation of the electron ellipsoids relative to the Ox axis, the asymptotes α_{ik} and σ_{ik} are as follows:[9,19]

$$\alpha_{23} \propto H, \quad \alpha_{22} \propto H, \text{но } \alpha_{23}(H) \neq \alpha_{32}(-H), \quad \alpha_{33} \propto H, \quad \sigma_{23}(H) = \sigma_{32}(H) \propto H^{-2}.$$

Equation (1) follows from (A.2) in this case.

[1] C. F. Gallo, R. C. Miller, P. H. Sutter and R. W. Ure, J. Appl. Phys. 33, 3144 (1962).

[2] E. Grüneisen, K. Rausch, K. Weiss, Ann. Physik 7, 1 (1950). G. K. White, S. B. Woods, Phil. Mag. 3, 342 (1958). W. C. Kaye and W. F. Higgins, Phil. Mag. 7, 1956 (1929). H. E. Banta, Phys. Rev. 41, 239 (1932), E. J. Knap, Phys. Rev. 39, 550 (1932). H. Reddeman, Ann. d. Phys. 20, 441 (1934). M. T. Rodine, Phys. Rev. 46, 910 (1934). W. J. de Haas, A. N. Gerritsen and W. H. Capel, Physica 3, 1143 (1936).

[3] C. F. Gallo, B. S. Chandrasekhar and P. H. Sutter, J. Appl. Phys. 34, 144 (1963).

[4] S. M. Bhagat and D. D. Manchon, Phys. Rev. 164, 66 (1967).

[5] J. Ziman, Electrons and Phonons (Oxford, 1957).

[6] E. L. Nagaev, FMM 25, 177 (1968).
[7] L. A. Fabelinskiĭ, Usp. Fiz. Nauk 94, 3 (1968) [Sov. Phys.-Uspekhi 11, 1 (1968)].
[8] J. L. Yarnell, J. L. Warren, R. G. Wenzel and S. H. Koenig, IBM J. Res. Develop. 8, 234 (1964).
[9] I. Ya. Korenblit, Fiz. Tekh. Poluprov. 2, 1425 (1968) [Sov. Phys.-Semicond. Semicond. 2, 1192 (1969)].
[10] Yi Han Kao, Phys. Rev. 129, 1122 (1963).
[11] L. S. Lerner, Phys. Rev. 127, 1480 (1962).
[12] S. Katsuki, M. Tsuji, J. Phys. Soc. Japan 25, 1193 (1968), S. Inoue and M. Tsuji, J. Phys. Soc. Japan 22, 1191 (1967). K. Walther, Phys. Rev. 174, 782 (1968).
[13] Y. Eckstein, A. W. Lawson, and D. H. Reneker, J. Appl. Phys. 31, 1534 (1960).
[14] A. Friedman, Phys. Rev. 159, 553 (1967).
[15] R. L. Hartman and S. H. Koenig, Bull. Am. Phys. Soc. 13, 383 (1968).
[16] A. A. Lopez, Phys. Rev. 175, 553 (1967).
[17] V. F. Gantmakher and Yu. S. Leonov, ZhETF Pis. Red. 8, 264 (1968) [JETP Lett. 8, 162 (1968)].
[18] C. Herring, Bell Syst. Tech. J. 34, 237 (1955).
[19] T. C. Harman, J. M. Honig and B. M. Tarmy, Adv. Energy Conv. 5, 1 (1968).
[20] I. Ya. Korenblit, M. E. Kuznetsov and S. S. Shalyt, Zh. Eksp. Teor. Fiz. 56, 8 (1969) [Sov. Phys.-JETP 29, 4 (1969)].

Translated by R. T. Beyer
214